

## Solid-State Complexes of Hexafluoro-2-propanol with Benzophenone-Containing Polyimides

G. K. Sturgill,<sup>†,§</sup> C. Stanley,<sup>‡</sup> M. E. Rezac,<sup>†</sup> and H. W. Beckham<sup>\*,‡</sup>

*School of Chemical Engineering and School of Textile and Fiber Engineering, Georgia Institute of Technology, Atlanta, Georgia 30332*

*Received December 5, 2000*

**ABSTRACT:** Films of benzophenone-containing polyimides were cast from hexafluoro-2-propanol (HFIP) solutions and vacuum-dried just above the HFIP boiling temperature (59 °C) until a constant weight was achieved. Upon heating, the films exhibited 15% weight loss beginning around 150 °C. Using infrared spectroscopy, it was determined that the evolved gas was HFIP, and it formed a hydrogen-bonded solid-state complex with the polyimide. The films still contained nearly 15% HFIP 18 months after casting, a testament to the room temperature stability of the complex. The HFIP-complexed polyimide films exhibited higher gas permeabilities and reduced selectivities compared to the same polyimide cast from dimethylformamide. These transport properties were attributed to plasticization of the polyimide by the HFIP, as evidenced by a reduced storage modulus and glass transition temperature compared to the uncomplexed polyimide.

Polyimides are commercially important polymers due partly to their chemical intractability. Since this property conflicts with high solubility, most polyimides are processed in their precursor polyamic acid form and later cured to generate the imide linkages along the backbone. Polyamic acids dissolve in a variety of solvents, some of which form stable complexes via hydrogen bonding with the –OH or –NH groups of the amic acid linkages.<sup>1</sup> Since this complexation can affect the imidization process and resultant polyimide properties, it has been the focus of numerous studies.<sup>1–3</sup> The following solvents are known to complex polyamic acids: dimethylformamide, dimethylacetamide,<sup>4</sup> 1-methyl-2-pyrrolidinone, and dimethyl sulfoxide. Dried, stable, solid-state complexes have been shown to contain up to 30% solvent on a weight basis.<sup>1</sup> High-temperature thermal annealing results in decomplexation and imidization to form the insoluble polyimide.

Evolution of volatiles accompanies thermal curing of polyamic acids which can lead to microvoid formation,<sup>5</sup> a possible defect for a polyimide employed in a gas-separation membrane. Thermal curing can also collapse porous substructures in polymers processed into asymmetric membrane structures. Thus, for applications in gas-separation membranes, some advantages exist for those polyimides that can be processed as polyimides. Accordingly, a variety of repeat-unit structures have been incorporated into polyimides to impart solubility and thus processability.<sup>6</sup> Even so, many of these polyimides remain relatively insoluble. One solvent often used for difficult-to-dissolve polymers is 1,1,1,3,3,3-hexafluoro-2-propanol (hexafluoro-2-propanol, or HFIP).<sup>7</sup> This strong hydrogen-bond donor ( $pK_a \sim 9.30$ ) easily solvates materials containing hydrogen-bond acceptor groups.<sup>8</sup> Such strong interactions can also lead to formation of stable complexes. Evidence of HFIP complexation has been clearly shown in liquids using a variety of spectroscopic techniques.<sup>9–11</sup> For example, the NMR chemical shift of the HFIP hydroxylic proton is

2.60 ppm in dilute carbon tetrachloride but 8.30 ppm in dimethylformamide (10% concentration); hydrogen-bond formation with dimethylformamide results in the large (5.70 ppm) downfield shift for the NMR signal of the HFIP hydroxylic proton.<sup>8</sup> Such strong hydrogen-bonding tendency has been synthetically incorporated into polymers via side-group hexafluorodimethylcarbinol functional groups for blend compatibilization<sup>12</sup> and sensor applications.<sup>13</sup>

Small molecules can remain complexed with polymers in the solid state, typically modifying a variety of physical properties. For example, *N,N*-dimethylacetamide and sulfonated poly(phenylene oxide) form a strong solid-state complex that exhibits reduced strength and stiffness, higher extensibility, and higher gas permeability.<sup>14</sup> Indeed, complexes have been designed and fabricated for improving gas transport properties of polymeric materials. Permeability and O<sub>2</sub>/N<sub>2</sub> selectivity of poly(methyl methacrylate), polycarbonate, and ionic polyurethane membranes are improved by complexation with dimethylformamide/metal salt mixtures.<sup>15–17</sup>

Efforts to improve gas-separation membranes also include cross-linking the polymeric matrix to increase thermal and chemical stability and influence transport properties. Continuing developments in this area have focused on the use of cross-linkable acetylene-terminated monomers and diacetylene-containing oligomers as minor components of polyimide blends.<sup>18–20</sup> For cross-linkable oligomers and host polyimides based on 3,3',4,4'-benzophenonetetracarboxylic anhydride (BTDA), a common solvent is HFIP. Complexation of HFIP with BTDA-based polyimides was examined with thermal and spectroscopic analyses. These results are reported in the following along with gas transport properties of the solid-state complex.

### Experimental Section

**Material Preparation.** Two benzophenone-containing polyimides were used in this study and will be referred to by their commercial names (see Figure 1). P84 was obtained from Lenzing (Austria) as a 25 wt % solution in DMF, and Matrimid

<sup>†</sup> School of Chemical Engineering.

<sup>‡</sup> School of Textile and Fiber Engineering.

<sup>§</sup> Current address: DuPont Nonwovens, Old Hickory, TN.

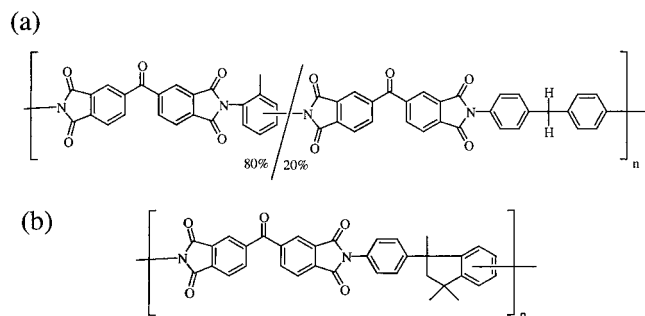


**Figure 1.** Repeat-unit structures of the benzophenone-containing polyimides known commercially as (a) P84 and (b) Matrimid.

was obtained as a powder from Ciba-Geigy. 1,1,1,3,3,3-Hexafluoro-2-propanol (Aldrich, 99.8+% purity) was used as received. To isolate the P84 as a solid, the DMF solution was cast on a glass plate to give films approximately 25  $\mu\text{m}$  thick. These films were dried in a vacuum oven at 150  $^{\circ}\text{C}$  until a constant weight was obtained. Dried P84 films or Matrimid powder was dissolved in HFIP to give a 5 wt % solution which was filtered through 0.45  $\mu\text{m}$  filters into casting rings in a nitrogen-purged glovebox at 24  $^{\circ}\text{C}$  and allowed to sit covered for 4 days before removal. These films were then placed in a vacuum oven at 60  $^{\circ}\text{C}$  for 48 h.

**Thermal Analysis.** Thermogravimetric analyses were conducted at 10  $^{\circ}\text{C}/\text{min}$  in a nitrogen atmosphere using a Setaram TGA/DSC 111 module or at a heating rate of 18  $^{\circ}\text{C}/\text{min}$  on a Seiko TG/DTA 320. Thermomechanical analysis was performed using a Seiko DMS 210; films were tested at 10 Hz as the temperature was ramped to 500  $^{\circ}\text{C}$  at a rate of 18  $^{\circ}\text{C}/\text{min}$ . Differential scanning calorimetry was conducted on a Seiko DSC 220 in a nitrogen stream ( $\sim 150$  mL/min) at a heating rate of 10  $^{\circ}\text{C}/\text{min}$ .

**Spectroscopic Analysis.** Using a Bruker Vector 22, Fourier transform infrared spectroscopy (FTIR) was conducted in transmission mode on either the 25  $\mu\text{m}$  thick solvent-cast films or on thin layers cast from HFIP solutions directly onto a salt plate (NaCl, 25  $\times$  4 mm). Prior to measurement, the salt-plate films were placed in a vacuum oven for 24 h at 60  $^{\circ}\text{C}$ . Evolved gas analysis (EGA) was carried out using a Nicolet FT-IR spectrometer attached to a nitrogen-purged furnace. The furnace was preheated to 250  $^{\circ}\text{C}$ , and the sample was quickly introduced.

**Gas Transport Analysis.** A constant volume/variable pressure apparatus was used to measure pure gas permeability coefficients for He (99.997%),  $\text{H}_2$  (99.995%),  $\text{N}_2$  (99.999%),  $\text{O}_2$  (99.8%),  $\text{CO}_2$  (99.8%), and  $\text{CH}_4$  (99%). All gases (Air Products) were used as received. The permeation cell was maintained at  $35 \pm 0.1$   $^{\circ}\text{C}$ . The feed pressure was  $10 \pm 0.05$  atm. On the permeate side of the film, the gas pressure was less than 10 Torr and considered negligible. The leak rate into the vacuum system introduced an error for the permeability measurements of less than 0.01% for the slowest gas. These techniques have been described in greater detail elsewhere.<sup>21</sup> Films used in gas permeation studies were approximately 25  $\mu\text{m}$  thick. Permeability errors are reported with the respective transport values. Error associated with the reported selectivities is not more than  $\pm 4\%$ .

## Results and Discussion

**Complex Characterization.** The benzophenone-containing polyimide P84 (see Figure 1) is provided as a solution in DMF, so films are naturally prepared by casting from this solvent. Following casting, the films were dried in a vacuum oven at 150  $^{\circ}\text{C}$  until they exhibited a constant weight. Since DMF boils at 153  $^{\circ}\text{C}$ , it was effectively removed by this drying procedure as evidenced by the TGA curve shown in Figure 2. The DMF-cast films showed the typical thermal behavior for

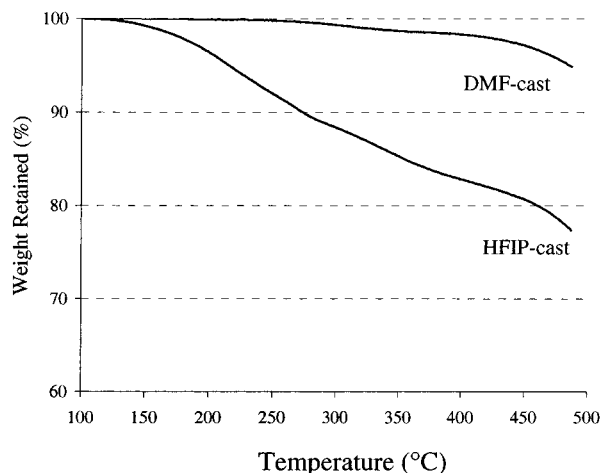


**Figure 2.** Residual mass as a function of temperature for solid P84 films cast from DMF and from HFIP. Prior to testing, the DMF-cast film was vacuum-dried at 150  $^{\circ}\text{C}$  ( $T_{\text{boil}}$  for DMF = 153  $^{\circ}\text{C}$ ) and the HFIP-cast film was vacuum-dried at 60  $^{\circ}\text{C}$  ( $T_{\text{boil}}$  for HFIP = 59  $^{\circ}\text{C}$ ). Measured in nitrogen at 10  $^{\circ}\text{C}/\text{min}$ .

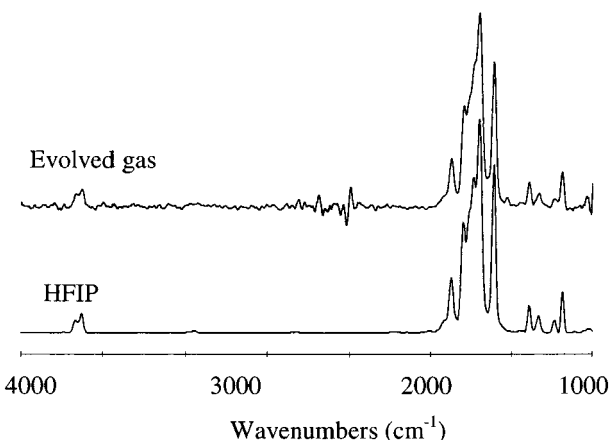


**Figure 3.** IR spectrum from evolved gas analysis of HFIP-cast P84 compared to the IR spectrum of HFIP (gas).

a polyimide, exhibiting little weight loss until 300  $^{\circ}\text{C}$ . The dried films were redissolved in HFIP. Films were cast, allowed to sit at 24  $^{\circ}\text{C}$  for 4 days, and then vacuum-dried at 60  $^{\circ}\text{C}$  to remove residual HFIP that boils at 59  $^{\circ}\text{C}$ . However, the TGA curve for the HFIP-cast film (see Figure 2) suggested a large fraction of the solvent was not removed; significant weight loss began around 150  $^{\circ}\text{C}$  and reached 12% at 300  $^{\circ}\text{C}$  and over 16% at 400  $^{\circ}\text{C}$ .

The identity of the evolved gas was verified with infrared spectroscopy. An HFIP-cast film was placed in an oven preheated to 250  $^{\circ}\text{C}$  that was flushed by a nitrogen stream and connected to the sampling chamber of an infrared spectrometer. The spectrum of the evolved gas is shown in Figure 3 along with the IR spectrum of HFIP. The weight loss observed in the TGA curves is clearly due to residual HFIP. The weight loss at 250  $^{\circ}\text{C}$  for films cast at the same time is plotted as a function of time after casting in Figure 4. Even after 18 months, the films still contain nearly 15% HFIP. While slightly more HFIP was retained during the first month, the weight loss stabilized at  $15 \pm 1.5\%$  by the second month.

In an attempt to examine whether the mass-loss profile (Figure 4) could be the result of a very small diffusion coefficient (due to the rather large size of HFIP), mass-loss profiles were generated<sup>22</sup> assuming Fickian diffusion from 25  $\mu\text{m}$  thick polymer films using

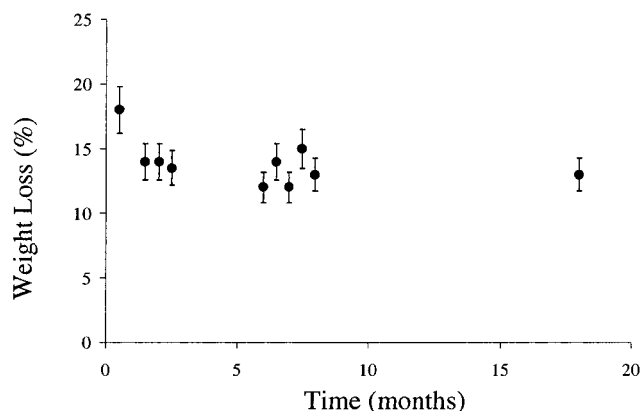


**Figure 4.** Weight loss as a function of time for HFIP-cast P84 films. The weight loss was determined by thermogravimetric analysis and taken as the value at 250 °C. Measured in nitrogen at 10 °C/min.

diffusion coefficients ranging from  $10^{-9}$  to  $10^{-17}$  cm<sup>2</sup>/s. Using a single value for the diffusion coefficient, none of these simulated profiles adequately described the experimental mass-loss profile shown in Figure 4. However, during the first month after casting, the initial mass loss may indeed be Fickian with a diffusion coefficient of approximately  $10^{-13}$  cm<sup>2</sup>/s. Following this period, the HFIP loss from the polyimide film stabilizes; such behavior is not expected from purely diffusive loss. In fact, assuming a diffusion coefficient of  $1.3 \times 10^{-13}$  cm<sup>2</sup>/s, 99% of a penetrant should be removed from a 25  $\mu$ m thick polymer film in about 2 months. These results suggest the presence of both free HFIP, which exhibits a diffusion coefficient of approximately  $10^{-13}$  cm<sup>2</sup>/s and is lost during the first month after casting, and bound HFIP, which exhibits a diffusion coefficient of approximately zero.

Of course, diffusion coefficients decrease with increasing molecular size of penetrants. Data are often reported for diffusion coefficients as a function of molar volume; one such set of data for glassy poly(vinyl chloride)<sup>23</sup> suggests that HFIP, with a molar volume of 105 cm<sup>3</sup>/mol, would exhibit a diffusion coefficient between  $10^{-14}$  and  $10^{-13}$  cm<sup>2</sup>/s through this polymer. The diffusion coefficient simulated for diffusive loss of free HFIP from the glassy P84 polyimide (i.e., during the first month after film casting) fits within this range. Thus, while free HFIP leaves the polyimide film at a rate consistent with its rather large molecular size, the residual HFIP does not and therefore must be bound to the polyimide matrix.

The solid-state interaction between HFIP and the benzophenone-containing polyimides was investigated with FTIR spectroscopy. Characteristic imide ring absorption bands are seen in the P84 spectrum: the imide carbonyl stretch (imide I) is observed at 1780 cm<sup>-1</sup> (symmetric) and 1720 cm<sup>-1</sup> (asymmetric), 1370 cm<sup>-1</sup> is attributed primarily to the C–N stretch (imide II), 1100 cm<sup>-1</sup> to C–N–C bending (imide III), and 730 cm<sup>-1</sup> to imide ring deformation (imide IV).<sup>24–26</sup> Other absorptions of note include a shoulder band at 1670 cm<sup>-1</sup> attributed to the benzophenone carbonyl and the phenylene carbon–carbon stretch at 1510 cm<sup>-1</sup>. This latter peak appears identical in the spectra of P84 and its complex with HFIP. However, subtle differences appear for all of the absorptions associated with the imide ring, thus suggesting some degree of interaction between the imide ring and HFIP.

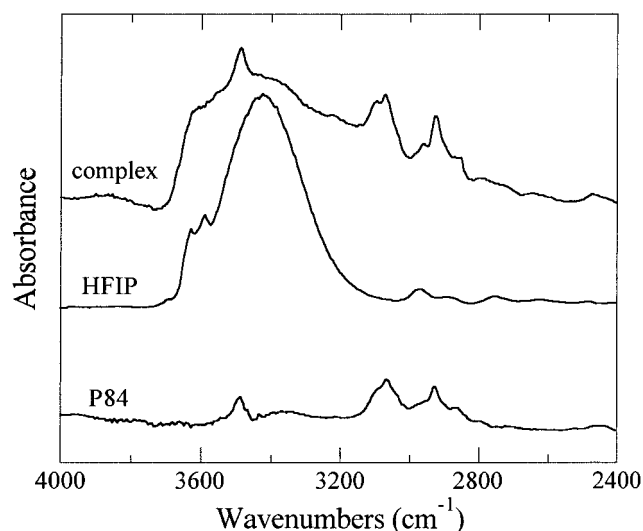


**Figure 5.** IR spectra of HFIP (neat liquid), P84, and the HFIP/P84 complex. The P84 and complex were both solid films cast onto KBr plates.

The O–H stretching region is shown in Figure 5 for HFIP, P84, and the HFIP/P84 complex. First, compare this region of the IR spectrum for liquid HFIP (Figure 5) with the same region for gaseous HFIP (Figure 3). In Figure 3, the O–H stretch of gaseous HFIP appears as a relatively sharp doublet centered at 3600 cm<sup>-1</sup>, observed previously for HFIP highly diluted in carbon tetrachloride and indicative of free HFIP.<sup>27,28</sup> In Figure 5, the O–H stretch for liquid HFIP is dominated by a much broader peak extending from 3200 to 3600 cm<sup>-1</sup> due to intermolecular hydrogen bonding. In the same figure, the O–H stretching region for the HFIP/P84 complex also shows a broad peak that actually extends below 3200 cm<sup>-1</sup>; this region cannot be reproduced by a simple linear combination of HFIP and P84 IR spectra. The same general differences and similarities were observed for the IR spectra of Matrimid and HFIP-cast Matrimid. The presence of hydrogen-bonded HFIP is thus clearly evident in the HFIP/polyimide complexes. Coupled with the mass-loss profile that provides evidence of HFIP bound to the polyimide matrix, these IR data indicate the formation of a hydrogen-bonded HFIP/polyimide complex.<sup>29</sup>

If a HFIP-cast P84 film is annealed under vacuum at 180 °C for 3 days, the IR spectrum of the film appears identical to the IR spectrum of the P84. The heating rate for decomplexation, however, affects the resulting film clarity. Upon casting from either DMF or HFIP, the polyimide films were yellow and transparent. If the HFIP-cast films were heated slowly (5 °C/min ramp to 180 °C, hold for 3 days), they remained yellow and transparent just like the DMF-cast films. If they were heated rapidly (placed in oven preheated to 220 °C), they became light brown and opaque. Examination with scanning electron microscopy (see Figure 6) revealed a microporous network for the rapidly decomplexed HFIP-cast films. Slow removal of the complexed HFIP ensures that the film remains dense and thus suitable for gas-separation applications.

**Gas Transport Properties.** The gas transport properties of three polyimide samples were evaluated: DMF-cast P84, HFIP-complexed P84, and P84 cast from HFIP and subsequently decomplexed by slow heating to 180 °C. The single-gas permeabilities measured at 35 °C and



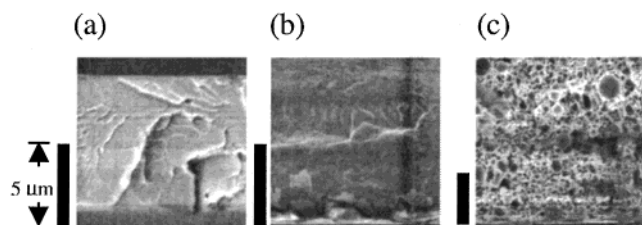


**Figure 6.** Scanning electron micrographs of (a) DMF-cast P84, heated to 180 °C, held 3 days, and then 4 h at 240 °C; (b) HFIP-cast P84, heated to 180 °C, held 3 days, and then 4 h at 240 °C; (c) HFIP-cast P84, placed in oven preheated to 220 °C for 5 min. Solid bar in lower left corner of each micrograph denotes 5  $\mu\text{m}$ .

**Table 1.** Gas Permeability and Ideal Selectivity for P84 and the HFIP/P84 Complex (10 atm Feed Pressure, 0 atm Permeate, 35 °C)

gas <sup>a</sup>	DMF-cast P84 (Ba) <sup>b</sup>	HFIP-complexed P84 (Ba) <sup>c</sup>	HFIP-cast, decomplexed P84 (Ba) <sup>c</sup>
H <sub>2</sub>	6.6 $\pm$ 0.18	9.3 $\pm$ 0.8	6.9 $\pm$ 0.56
He	7.9 $\pm$ 0.22	12.0 $\pm$ 1.1	8.7 $\pm$ 0.7
CO <sub>2</sub>	0.9 $\pm$ 0.02	4.9 $\pm$ 0.4	1.2 $\pm$ 0.1
O <sub>2</sub>	0.28 $\pm$ 0.008	1.2 $\pm$ 0.1	0.35 $\pm$ 0.03
N <sub>2</sub>	0.034 $\pm$ 0.001	0.22 $\pm$ 0.02	0.046 $\pm$ 0.004
CH <sub>4</sub>	0.017 $\pm$ 0.001	0.18 $\pm$ 0.02	0.025 $\pm$ 0.002
ideal selectivity			
H <sub>2</sub> /CH <sub>4</sub>	388 $\pm$ 34	52 $\pm$ 10	276 $\pm$ 45
CO <sub>2</sub> /CH <sub>4</sub>	53 $\pm$ 4	27 $\pm$ 5	48 $\pm$ 8
O <sub>2</sub> /N <sub>2</sub>	8.2 $\pm$ 0.5	5.5 $\pm$ 1.0	7.6 $\pm$ 1.3

<sup>a</sup> 1 Ba = 1 barrer =  $10^{-10}$  [cm<sup>3</sup>(STP) cm]/[cm<sup>2</sup> s cmHg]. <sup>b</sup> Knife-drawn. <sup>c</sup> Ring-cast.

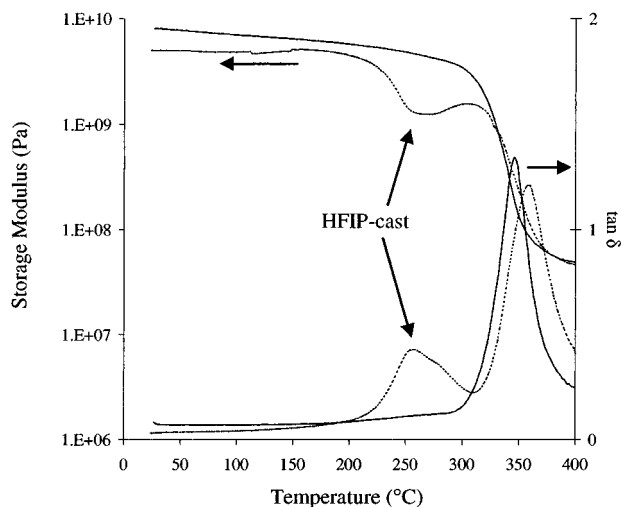


**Figure 7.** Dynamic mechanical storage moduli and loss tangents (10 Hz) as a function of temperature for DMF-cast P84 (solid lines) and HFIP-complexed P84 (dashed lines). Analysis completed in nitrogen with an 18 °C/min heating rate.

10 atm feed pressure are presented in Table 1 along with ideal selectivities for three gas pairs.

The HFIP-complexed P84 exhibits marked increases in single-gas permeabilities with corresponding losses in ideal selectivities as compared to the DMF-cast P84. These permeability increases are attributed to plasticization, well-known to cause permeability increases in a variety of polymers.<sup>14,30</sup> Evidence for plasticization of the polyimide by the complexed HFIP is revealed in the dynamic mechanical data of Figure 7; storage moduli and loss tangents are plotted vs temperature for the

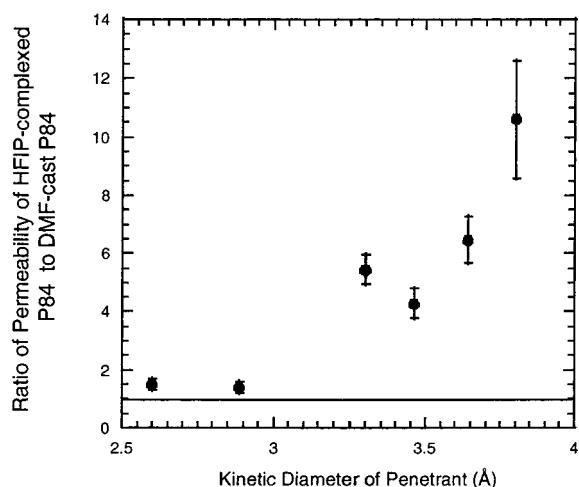


**Figure 8.** Ratio of the permeability of gases through HFIP-complexed P84 to DMF-cast P84 as a function of the kinetic diameter of the penetrant. All gas permeabilities were measured at 10 atm feed pressure, 35 °C.

DMF-cast and the HFIP-complexed P84. The HFIP-complexed P84 exhibits a reduced modulus and decreased glass transition compared to the DMF-cast polymer. The bound fluorinated alcohol apparently reduces segmental interactions and increases average interchain spacings, resulting in reduction of the glass transition from 350 to about 250 °C. However, since the HFIP is decomplexed when the sample is heated above 150 °C (see Figure 2), it is clearly evaporating from the sample during the dynamic mechanical testing. Consequently, the glass transition at 250 °C never fully develops, and the associated drop in the storage modulus levels off. Above 250 °C, the storage modulus increases, reflecting the deplasticization accompanying HFIP loss, until the glass transition of the unplasticized P84 is reached. The glass transition of the now-unplasticized P84 is distinguished by a second  $\tan \delta$  peak at 360 °C. It appears about 10 °C higher than the  $T_g$  for the DMF-cast P84 due to the HFIP-assisted sub- $T_g$  annealing that occurs before HFIP loss.

The extent to which the HFIP-complexed P84 exhibits increased gas permeabilities is directly related to the size of the penetrant molecule. Figure 8 shows the ratio of the permeability of the HFIP-complexed P84 relative to the DMF-cast material as a function of the penetrant size, presented here as the kinetic diameter.<sup>31</sup> As the size of the penetrant increases, the transport properties are more strongly influenced by the presence of the complexed solvent. Dramatic increases for the large gases, with less significant changes in the small gas permeabilities, have been previously reported for plasticized systems<sup>32</sup> and attributed to higher diffusivities resulting from increased segmental mobilities. Removal of the HFIP through a controlled slow thermal treatment results in reductions in permeabilities, but the absolute permeabilities of the decomplexed P84 (shown in Table 1) are still slightly higher than those of the DMF-cast P84 (except for hydrogen and helium, which are statistically equivalent). These higher permeabilities are attributed to the conditioning of the polyimide by the presence of the small-molecule penetrant,<sup>33,34</sup> HFIP. The HFIP is accommodated by the polyimide segments and then removed by slow heating to 180 °C for 3 days and then for 4 h at 240 °C; the temperature is never raised above the glass transition, and therefore complete

segmental relaxation does not occur. The HFIP is completely removed according to TGA measurements, but the polyimide segments maintain some degree of structural positioning that allows higher diffusivities as compared to that of the DMF-cast P84.

## Conclusions

High-quality films of benzophenone-containing polyimides can be cast from solutions of the polymers in hexafluoro-2-propanol (HFIP). Vacuum-drying of the solid films just above the boiling point of the solvent (59 °C) did not completely remove the HFIP due to the formation of a hydrogen-bonded complex. Thermogravimetric analysis revealed the HFIP could be thermally driven off beginning around 150 °C. The mass fraction of HFIP in the films stabilized around 15% a few weeks after casting; 18 months after casting, the films still contained nearly 15% HFIP, demonstrating the room temperature stability of the complex.

The HFIP-complexed polyimide films exhibited higher gas permeabilities and reduced selectivities compared to the same polyimide cast from dimethylformamide. These transport properties were attributed to plasticization of the polyimide by the HFIP, as evidenced by a reduced storage modulus and glass transition temperature compared to those of the uncomplexed polyimide. Note that only a single concentration of HFIP was examined here (15 wt %); it is unclear how other levels of HFIP incorporation in a polyimide would affect the modulus, glass transition, and transport properties. It is clear, however, that polyimide membranes prepared from HFIP-containing solvent mixtures could contain significant fractions of hydrogen-bonded HFIP unless proper drying procedures are implemented, and such residual solvent affects the gas transport properties.

**Acknowledgment.** Thanks are extended to Jon Crate of the Georgia Tech Research Institute for assistance with EGA and Linda Herrera for FTIR. Portions of this work were supported by the Environmental Protection Agency under agreement R824727 and the National Science Foundation under grant CTS-9806004. Kip Sturgill gratefully acknowledges partial fellowship support provided by the Georgia Tech Molecular Design Institute, under prime contract N00014-95-1-1116 from the Office of Naval Research.

## References and Notes

- (1) Laius, L. A.; Tsapovetsky, M. I. In *Polyamic Acids and Polyimides: Synthesis, Transformations and Structure*; Besonov, M. I., Zubkov, V. A., Eds.; CRC Press: Boca Raton, FL, 1993.
- (2) Dine-Hart, R. A.; Wright, W. W. *J. Appl. Polym. Sci.* **1967**, *11*, 609.
- (3) (a) Brekner, M. J.; Feger, C. *J. Polym. Sci., Part A: Polym. Chem.* **1987**, *25*, 2005. (b) *J. Polym. Sci., Part A: Polym. Chem.* **1987**, *25*, 2479.
- (4) Bower, G. M.; Frost, L. W. *J. Polym. Sci., Part A* **1963**, *1*, 3135.
- (5) Bruma, M.; Schulz, B.; Mercer, F. W. *Polymer* **1994**, *35*, 4209.
- (6) Huang, S. J.; Hoyt, A. E. *Trends Polym. Sci.* **1995**, *3*, 262.
- (7) Costa, G.; Russo, S. *J. Macromol. Sci., Chem.* **1982**, *A18*, 299.
- (8) Middleton, W. J.; Lindsey, Jr., R. V. *J. Am. Chem. Soc.* **1964**, *82*, 4948.
- (9) Juršić, B.; Ladika, M.; Sunko, D. E. *Tetrahedron Lett.* **1985**, *26*, 5323.
- (10) Ladika, M.; Juršić, B.; Sunko, D. E. *Spectrochim. Acta* **1986**, *42*, 1397.
- (11) Ganguly, T.; Mal, S.; Mukherjee, S. *Spectrochim. Acta* **1983**, *39A*, 657.
- (12) Pearce, E. M.; Kwei, T. K.; Min, B. Y. *J. Macromol. Sci., Chem.* **1984**, *A21*, 1181.
- (13) Snow, A. W.; Sprague, L. G.; Soulen, R. L.; Grate, J. W.; Wohltjen, H. *J. Appl. Polym. Sci.* **1991**, *43*, 1659.
- (14) Polotskaya, G. A.; Agranova, S. A.; Antanova, T. A.; Elyashovich, G. K. *J. Appl. Polym. Sci.* **1997**, *66*, 1439.
- (15) Lai, J.-Y.; Huang, S.-J.; Chen, S.-H. *J. Membr. Sci.* **1992**, *74*, 71.
- (16) Lai, J.-Y.; Chen, S.-H.; Lee, M.-H.; Shyu, S. S. *J. Appl. Polym. Sci.* **1993**, *47*, 1513.
- (17) Huang, S.-L.; Chao, M.-S.; Lai, J.-H. *J. Appl. Polym. Sci.* **1998**, *67*, 865.
- (18) Rezac, M. E.; Sorensen, E. T.; Beckham, H. W. *J. Membr. Sci.* **1997**, *136*, 249.
- (19) Rezac, M. E.; Schöberl, B. *J. Membr. Sci.* **1999**, *156*, 211.
- (20) Bayer, B.; Schöberl, B.; Nagapudi, K.; Rezac, M. E.; Beckham, H. W. In *Polymer Membranes for Gas and Vapor Separation*; Freeman, B. D., Pinnau, I., Eds.; ACS Symposium Series 733; American Chemical Society: Washington, DC, 1999; Chapter 17.
- (21) O'Brien, K. C.; Koros, W. J.; Barbari, T. A.; Sanders, E. S. *J. Membr. Sci.* **1986**, *29*, 229.
- (22) Crank, J. *The Mathematics of Diffusion*; Clarendon: Oxford, 1986.
- (23) Baker, R. *Membrane Technology and Applications*; McGraw-Hill: New York, 2000; p 292.
- (24) Dine-Hart, R. A.; Wright, W. W. *Makromol. Chem.* **1971**, *143*, 189.
- (25) Ishida, H.; Wellinghoff, S. T.; Baer, E.; Koenig, J. L. *Macromolecules* **1980**, *13*, 826.
- (26) Pryde, C. A. *J. Polym. Sci., Part A: Polym. Chem.* **1989**, *27*, 711.
- (27) Barlow, J. W.; Cassidy, P. E.; Lloyd, D. R.; You, C.-J.; Chang, Y.; Wong, P. C.; Noriyan, J. *Polym. Eng. Sci.* **1987**, *27*, 703.
- (28) Purcell, K. F.; Strikeleather, J. A.; Brunk, S. D. *J. Am. Chem. Soc.* **1969**, *91*, 4019.
- (29) Earlier reported as solvolysis. Sturgill, G. K.; Stanley, C.; Beckham, H. W.; Rezac, M. E. *Polym. Mater. Sci. Eng. (Prepr. Am. Chem. Soc., Div. Polym. Mater. Sci. Eng.)* **1999**, *80*, 201.
- (30) Sefcik, M. D.; Schaefer, J.; May, F. L.; Raucher, D.; Dub, S. M. *J. Polym. Sci., Polym. Phys.* **1983**, *21*, 1041.
- (31) Breck, D. W. *Zeolite Molecular Sieves*; Wiley: New York, 1974; p 636.
- (32) Petropoulos, J. H. *J. Membr. Sci.* **1992**, *75*, 47.
- (33) Wonder, A. G.; Paul, D. R. *J. Membr. Sci.* **1979**, *5*, 63.
- (34) Sefcik, M. D.; Schaefer, J. *J. Polym. Sci., Polym. Phys.* **1983**, *21*, 1055.

MA002072G